

---

# Neural Audio Codecs for Prompt-Driven Universal Source Separation

---

**Adhiraj Banerjee, Vipul Arora**

Department of Electrical Engineering  
Indian Institute of Technology  
Kanpur, India  
`{adhiraj, vipular}@iitk.ac.in`

## Abstract

Text-guided source separation supports flexible audio editing across media and assistive applications, but existing models like AudioSep are too compute-heavy for edge deployment. Neural Audio Codec-based models such as CodecFormer and SDCodec are compute efficient but limited to fixed-class separation. We introduce CodecSep, the first NAC-based model for on-device universal, text-driven separation. CodecSep combines DAC compression with a transformer masker modulated by CLAP-derived FiLM parameters. Across six open-domain benchmarks under matched training/prompt protocols, **CodecSep** surpasses **AudioSep** in separation fidelity (SI-SDR) while remaining competitive in perceptual quality (ViSQOL) and matching or exceeding fixed-stem baselines (TDANet, CodecFormer, SDCodec). In code-stream deployments, it needs just 1.35 GMACs end-to-end— $\sim 54 \times$  less compute ( $25 \times$  architecture-only) than spectrogram domain separators like AudioSep—while remaining fully bitstream-compatible.

## 1 Introduction

In this manuscript, we propose CodecSep, a novel framework for text-conditioned source separation that combines the interpretability of prompt-driven separation with the compute efficiency of neural audio codecs (NACs). CodecSep is the first model to bridge NACs with universal source separation (USS), enabling flexible extraction of arbitrary sound sources based on natural language queries. By conditioning a transformer-based masker on text embeddings generated via the text branch of CLAP—a multimodal encoder trained on audio-text pairs Wu et al. [2023]—CodecSep performs state-of-the-art (SOTA) separation directly in the NAC encoder latent space, introducing semantic control while maintaining very low compute cost.

The growing demand for flexible, real-time audio processing in bandwidth-constrained or on-device scenarios calls for generalizable and computationally efficient methods. Traditional separation models tackle the challenge of disentangling sound sources from complex mixtures Vincent et al. [2018] but are typically specialized for narrow domains such as speech or music. USS broadens this scope by separating arbitrary sources without reliance on predefined labels. Within this setting, text-guided source separation has emerged as a compelling approach, enabling users to specify the target source via natural language prompts—offering greater transparency, flexibility, and accessibility in real-world applications.

Recent advances have embraced this direction by integrating textual prompts into separation pipelines. Architectures based on the Conv-TasNet encoder-masker-decoder blueprint Luo and Mesgarani [2019] have achieved strong results in domain-specific tasks Chen et al. [2020b], Subakan et al. [2021], Li et al. [2023]. Systems like AudioSep Liu et al. [2024] extend this framework to the text-conditioned setting by encoding text queries with models such as BERT Devlin et al. [2019] or

CLAP Wu et al. [2023] and injecting semantic information through Feature-wise Linear Modulation (FiLM) layers Perez et al. [2018]. These modifications allow intermediate representations to adapt dynamically to prompt semantics, steering the model towards the desired source.

However, such models, trained with signal-level objectives like scale-invariant signal-to-distortion ratio (SI-SDR) Luo and Mesgarani [2019], Le Roux et al. [2019], are not only highly sensitive to compression artifacts but also tend to be large and computationally intensive. This limits their practicality for on-device or real-time applications where resources are constrained. As a result, they are often deployed via the cloud, introducing additional latency and infrastructure costs.

Neural audio codecs (NACs) offer a promising alternative. Models like SoundStream Zeghidour et al. [2022], Encodec Défossez et al. [2022], and DAC Kumar et al. [2023] compress audio into discrete token sequences using encoder-quantizer-decoder pipelines. Leveraging Residual Vector Quantization (RVQ), they enable adaptive bitrate control and efficient representation. These codecs are trained on diverse audio data using a combination of adversarial and perceptual losses, which promotes both fidelity and robustness under compression. The resulting token representations have proven useful in tasks such as audio generation for multimodal models Wang et al. [2024], Du et al. [2024] and language-conditioned synthesis Borsos et al. [2023], Wang et al. [2023]. Building on this foundation, recent efforts like CodecFormer Yip et al. [2024b] and SDCodec Bie et al. [2024] have explored incorporating NACs into source separation pipelines. While these approaches achieve lightweight, high-fidelity performance, they remain limited to separating fixed types of sources (e.g., speech separation).

CodecSep addresses this gap by combining the computational efficiency of NACs with the flexibility of language-guided separation. It follows a NAC-based encoder-decoder architecture and integrates a transformer-based masker conditioned on CLAP-derived text embeddings. These embeddings generate FiLM parameters that modulate each transformer layer, enabling the model to selectively extract sources that align with the user’s query. Operating entirely in the codec latent space, CodecSep delivers interpretable, high-performance separation under strict computational constraints.

We evaluate CodecSep for universal source separation under a comprehensive set of protocols: (i) **dnr-v2** for in-domain text-guided separation; (ii) five *open-domain* corpora—AudioCaps, ESC-50, Clotho-v2, AudioSet-eval, and VGGSound—for cross-domain generalization; (iii) three *prompt granularities* (fixed-stem, generic three-stem {“speech”, “music”, “sfx”}, and a universal setting with fine-grained, compositional SFX descriptions); and (iv) *paraphrase robustness* via unseen synonyms for speech/music. We also include an *architectural ablation* contrasting decoder-style source generation (CodecFormer Yip et al. [2024b]) with our Transformer *masker* over codec latents, plus a reconstruction diagnostic (Appendix) to probe source leakage and mixture consistency.

To assess both quality and efficiency, we benchmark against the SOTA text-guided baseline, **AudioSep** Liu et al. [2024], under matched training data and prompt protocols. Across dnr-v2 and the open-domain benchmarks, CodecSep consistently surpasses AudioSep in SI-SDR while remaining competitive in ViSQOL, and it degrades more gracefully under prompt paraphrasing. In deployment-typical code-stream settings, CodecSep runs at just 1.35 GMACs end-to-end— $\sim 54\times$  less compute (and  $\sim 25\times$  architecture-only) than spectrogram-domain separators like AudioSep—while remaining fully compatible with bitstream interfaces.

## 2 Related Work

### 2.1 Audio Source Separation

Notable approaches like DPTNet Chen et al. [2020b], SepFormer Subakan et al. [2021], and TDANet Li et al. [2023] follow the encoder-masker-decoder framework. In this setup, the encoder generates STFT-like latent representations. At the same time, a masker network predicts source masks, which are then applied elementwise to the encoder outputs to obtain source-specific latent representations. These estimates are further processed by a decoder, which mirrors the encoder architecture, to reconstruct the source audio. TDANet Li et al. [2023], the latest iteration, enhances this framework with a top-down attention mechanism, using global and local attention modules to hierarchically model multi-scale acoustic features. CodecSep also adopts this encoder-masker-decoder structure, extending it to operate in the NAC latent space with text guidance.

Beyond the encoder-masker-decoder paradigm, a variety of alternative architectures have been explored. Models like Wave-UNet Stoller et al. [2018] and Demucs Défossez et al. [2019], Défossez et al. [2021] utilize encoder-decoder designs that estimate source waveforms directly, omitting the masking stage altogether. Other approaches operate in the frequency domain, notably, models like MM-DenseLSTM Takahashi et al. [2018], DCCRN Hu et al. [2020], and UNet-based architectures such as Spleeter Hennequin et al. [2020] perform separation directly in the complex STFT domain, jointly modelling magnitude and phase components. These diverse strategies highlight the broad design space of source separation, spanning both time and frequency domains, with and without masking.

## 2.2 Universal Source Separation

Prior work on source separation has concentrated mainly on speech or music-specific tasks. More recent advances have shifted toward USS, which aims to disentangle arbitrary sources from a mixture without assuming predefined source categories. Supervised USS models often employ Permutation Invariant Training (PIT) Yu et al. [2017], Kavalerov et al. [2019], while unsupervised approaches like Mixture Invariant Training (MixIT) Wisdom et al. [2020] learn directly from mixtures without access to clean references. However, both approaches assume a fixed maximum number of sources in the mixture and produce all outputs indiscriminately. As a result, an additional source identification step is needed post-separation to determine which of the estimated signals corresponds to the target source.

Query-Guided Source Separation (QSS) extends USS by enabling source extraction through external queries, including visual input, exemplar audio, class labels, or text. Text queries are particularly effective, offering a compact and expressive way to convey high-level semantics and encode spatial or temporal cues of the query source—all without the need for expensive reference data. Recent work such as AudioSep Liu et al. [2024] explores text-guided separation by integrating embeddings from models like BERT Devlin et al. [2019] and CLAP Wu et al. [2023], the latter of which aligns audio and text in a shared embedding space. AudioSep employs FiLM conditioning into the separation pipeline at intermediate layers of the masker. CodecSep adopts a similar strategy but operates in the NAC encoder latent space instead.

## 2.3 Source Separation with Neural Audio Codecs

Recent work has explored integrating neural audio codecs into source separation pipelines. CodecFormer Yip et al. [2024b] and its extension CodecFormer-EL Yip et al. [2024a] both leverage DAC as the encoder-decoder backbone, performing separation directly in the codec’s latent embedding space via a transformer-based separation module. The original CodecFormer is trained using a negative SI-SDR loss to supervise the predicted outputs. At the same time, CodecFormer-EL introduces an embedding-level objective that minimizes the distance between the separator’s output and the DAC encoder’s ground truth latent embeddings for each source. In contrast, SD-Codec Bie et al. [2024] integrates source separation more tightly into the codec itself. It is explicitly designed to disentangle mixtures into speech, music, and SFX. To achieve this, it introduces three dedicated RVQ branches—each trained to encode a specific source category. During encoding, the outputs of these domain-specific quantizers are summed across time to form a mixture-level representation, which is then decoded to reconstruct both the whole mixture and individual sources. This design enables SD-Codec to embed separation behavior directly into the codec’s structure. In this work, we repurpose the CodecFormer transformer separator into a text-conditioned mask predictor, enabling prompt-guided control over the separation process.

## 3 Method

CodecSep is based on the 16kHz variant of CodecFormer Yip et al. [2024b], which we adapt to enable text-driven source separation. Specifically, we modify the transformer module to function as a source mask estimator and incorporate Feature-wise Linear Modulation (FiLM) Perez et al. [2018] to inject text-based conditioning into the separation process. FiLM layers are applied to the transformer’s intermediate activations, allowing the model to adjust its internal representations based on the semantics of the input query. To produce the FiLM parameters, a lightweight query network

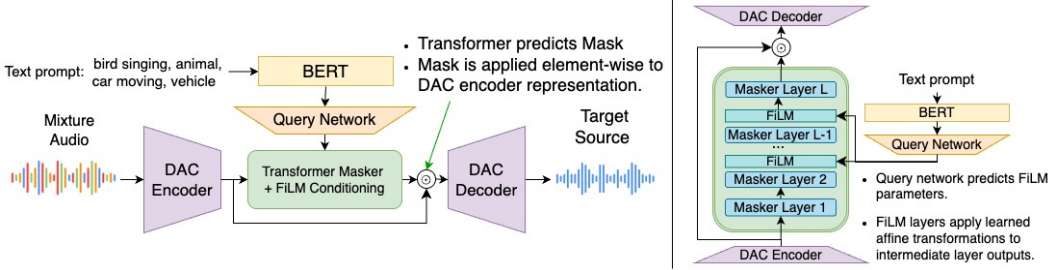


Figure 1: An overview of CodecSep. (Left) The full pipeline for text-guided USS. (Right) The integration of text conditioning into intermediate layers of transformer masker via FiLM layers.

consumes embeddings produced by a pretrained CLAP encoder Wu et al. [2023] from the input prompt.

Figure 1 (Left) illustrates our text-guided USS pipeline. Unlike AudioSep’s raw STFT-based, compute-heavy architecture, CodecSep operates on compact codec representations, offering significantly greater compute efficiency for resource-constrained edge deployment. Figure 1 (Right) illustrates how text-conditioning is integrated into the intermediate encoder layers of the transformer masker.

### 3.1 Model Architecture

CodecSep utilizes DAC Kumar et al. [2023] for the encoder-decoder modules and a transformer-based masker network with text conditioning to disentangle query sources within the DAC encoder representation space. We will discuss each component in detail and present how we incorporated text conditioning within the transformer masker architecture.

#### 3.1.1 Codec Backbone

DAC Kumar et al. [2023] builds upon the Encodenc Défossez et al. [2022] and SoundStream Zeghidour et al. [2022] architectures and utilizes fully convolutional encoder and decoder networks. Leaky ReLU activations in the architectures are substituted with the periodic Snake Activation function Ziyin et al. [2020] expressed as  $x + \sin^2 x$ . This enhances the modeling of periodic audio signals by incorporating a periodic inductive bias. Residual vector quantization is integrated into the encoder output, which enables audio compression at varying bit rates. In addition, factorized codes—where code assignment occurs in a lower-dimensional space than the codebook vectors—and L2-normalized codebook vectors are utilized to enhance codebook efficiency.

Let us consider compressing an audio recording  $x(t)$  of duration 1s, sampled at  $F_s = 24\text{kHz}$  to target bit-rate of  $R = 6000\text{bps}$ . The encoder network  $Enc(\cdot)$  down-samples  $x(t)$  by a factor of  $M = 320$  and outputs  $T = \frac{F_s}{M} = 75$  frames of latent representations, denoted as  $Z = [z_t \in R^d | t \in [T]]$ . Each frame  $z_t$  is allocated  $r = \frac{R}{T} = 80$  bits. Residual vector quantization (RVQ) efficiently allocates the bit-rate budget across a cascade of  $N_q = 8$  vector quantizers. The first vector quantizer in the cascade quantizes the frame  $z_t$ , and the residuals (the quantization error) are computed. The residuals are then iteratively quantized by the remaining  $N_q - 1$  quantizers in the cascade. Each quantizer is assigned  $r_i = \frac{r}{N_q} = 10$  bits, maintaining a manageable code-book size of  $2^{10} = 1024$ . The number of quantizers in the cascade  $N_q$  is key in balancing computational complexity and compression for a given bit-rate budget  $r$ .

The RVQ network  $Quant(\cdot)$  produces a code matrix  $A = [a_t \in [1024]^8 | t \in [T]]$  given encoder output  $Z$ . Each frame  $z_t \in Z$  is quantized into a code vector  $a_t \in [1024]^8$ , which can be mapped to an embedding via code-book lookup as  $e_t = \sum_{i=1}^8 e_t^i$ , where  $e_t^i$  corresponds to the embedding associated with code  $a_t^i \in [1024]$  from the  $i^{th}$  RVQ code-book. The RVQ output embedding sequence  $E = [e_t | t \in [T]]$  is then processed by the decoder network  $Dec(\cdot)$ , which up-samples it to generate  $y(t)$ , a reconstruction of the original audio  $x(t)$ .

### 3.1.2 Transformer Masker

CodecSep masker module  $Mask(\cdot)$  predicts source mask given DAC Kumar et al. [2023] encoder  $Enc(\cdot)$  representation  $Z$ . These masks are applied element-wise to representation  $Z$  to extract the corresponding source representation estimate. It follows CodecFormer Yip et al. [2024b] Transformer separator module architecture and is designed as a stack of  $L = 16$  transformer layers  $Mask^{l \in [L]}(\cdot)$  of embedding size  $d = 256$ . The output of the final transformer layer,  $H^L = Mask^L(H^{L-1})$ , is processed through  $K$  distinct 1D convolutional layers to generate source masks  $\{M_k | k \in [K]\}$ . To preserve the periodic inductive bias across the entire model, the Snake activation function, employed in DAC Kumar et al. [2023], replaces tanh and LeakyReLU activations throughout the masker module. The resulting source representation estimates are subsequently mapped to time domain  $\{\tilde{y}_k = Dec(M_k \odot Z) | k \in [K]\}$  using DAC Kumar et al. [2023] decoder  $Dec(\cdot)$  directly, without being processed by RVQ network  $Quant(\cdot)$ .

### 3.1.3 Text-guided Source Separation

We consider a single-channel audio mixture  $x(t) \in \mathbb{R}^{1 \times N}$ , which consists of an unknown number of overlapping open-domain sound sources. The mixture is expressed as the following sum:

$$x(t) = \sum_{s \in \mathcal{S}} y_s(t) \quad (1)$$

where  $\mathcal{S}$  is the (potentially unbounded) set of sound source classes or instances present in the mixture. Our objective is to recover a target source waveform or stem  $y_s(t)$  from the mixture  $x(t)$ , using a natural language query  $\tau_s$  that semantically describes the desired source. These prompts may reference specific sources (e.g., “dog barking,” “violin solo,” “crowd cheering”) or combinations of sources (e.g., “speech and music,” “footsteps and glass breaking”), allowing for fine-grained control.

To integrate text-based conditioning into CodecSep, we leverage CLAP Wu et al. [2023] and utilize a masker module  $Mask(\cdot)$  with  $K = 1$  final convolution to generate a single source mask  $M_s$ . Given a query text  $\tau$  that describes the target source, CLAP Wu et al. [2023] generates a corresponding text embedding  $e_\tau \in \mathbb{R}^d$ . This embedding is used to modulate the intermediate  $l \in [2, \dots, L-1]$  transformer layers  $Mask^l(\cdot)$  via feature-wise linear modulation (FiLM) Perez et al. [2018], enabling the network to estimate the desired source conditioned on the text input.

At transformer layer  $l$ , the layer output  $H^l \in \mathbb{R}^{d \times T}$  is modulated along the feature dimension using parameters  $\gamma^l, \beta^l \in \mathbb{R}^d$ . These modulation parameters are generated by a query network  $query(\cdot)$ , which processes text embedding  $e_\tau$  to produce  $(\gamma^l, \beta^l)_{l=1}^L = query(e_\tau)$ . The modulation transformation is then carried out as follows:

$$\tilde{H}_s^l = FiLM(H_i^l, \gamma_i^l, \beta_i^l) = \gamma_i^l H_i^l + \beta_i^l, \forall i \in [d] \quad (2)$$

The decoder network  $Dec(\cdot)$  subsequently processes the source representation estimate  $\tilde{Z}_s = M_s \odot Z$  and generates an estimate of the query source audio  $\tilde{y}_s = Dec(\tilde{Z}_s)$ .

## 3.2 Training Objective

We train CodecSep to reconstruct each individual source from mixtures using textual prompts corresponding to broad categories such as music, speech, and a wide range of sound effects (SFX). We also reconstruct the input mixture  $x$  by decoding the summed source latent estimates:  $\tilde{x} = g(\sum_s \tilde{Z}_s)$ . The model is optimized using the negative scale-invariant signal-to-distortion ratio (SI-SDR) loss Luo and Mesgarani [2019], Le Roux et al. [2019], encouraging the faithful separation of sources aligned with the given queries.

To support generalization across varied SFX types, prompts associated with SFX are not limited to atomic events—they may describe composite scenarios involving multiple overlapping sources (e.g., “footsteps, background traffic,” “crowd cheering, fireworks”), requiring the model to isolate multi-faceted acoustic scenes based on complex queries.

SI-SDR is designed to measure the similarity between the predicted  $\tilde{v}$  and ground truth  $v$  signals, focusing on the signal-to-noise ratio (SNR) while being invariant to scale differences. It is given as,

$$\text{SI-SDR}(v, \tilde{v}) = \sum_{k=1}^K 10 \log_{10} \frac{||\alpha v||^2}{||\alpha v - \tilde{v}||^2}, \alpha = \frac{\tilde{v}^T v}{||v||^2} \quad (3)$$

The overall loss function is then given as:

$$\mathcal{L} = - \sum_s \text{SI-SDR}(y_s, \tilde{y}_s) - \text{SI-SDR}(x, \tilde{x}) \quad (4)$$

To account for compression artifacts and improve training stability, we further compute the negative codec SI-SDR (cSI-SDR) Yip et al. [2024b], which is a variant of SI-SDR calculated with a codec-processed version of ground truth audio. During training, we keep the DAC Kumar et al. [2023] backbone and CLAP Devlin et al. [2019] text encoder weights frozen, updating only the parameters of  $Mask(\cdot)$  and  $query(\cdot)$  modules.

### 3.3 Design Rationale: FiLM-Conditioned Masking in NAC Latent Space

**Problem setup and pipeline contrast.** Let  $x(t) \in \mathbb{R}$  be a mono mixture with sources  $\{y_s(t) | s \in \mathcal{S}\}$ , where  $x(t)$  is expressed as equation 1.

**Spectrogram-domain (AudioSep):**

$$x \xrightarrow{\text{STFT}} X \in \mathbb{C}^{F \times T} \xrightarrow{g(X, e_\tau)} \tilde{Y}_s = |\hat{M}_s| \odot |X| \exp(\angle X + \angle \hat{M}_s) \xrightarrow{\text{ISTFT}} \tilde{y}_s(t),$$

where  $g(\cdot, e_\tau)$  denotes a FiLM-conditioned, complex-domain spectrogram separator that predicts a magnitude mask  $|\hat{M}_s| \in [0, 1]^{F \times T}$  and a phase residual  $\angle \hat{M}_s$ , conditioned jointly on the mixture spectrogram  $X$  (obtained by the STFT of  $x$ ) and the text embedding  $e_\tau$ . The predicted magnitude mask and phase residual are then applied element-wise to form the source spectrogram  $\tilde{Y}_s$  which is subsequently transformed back to the time domain via ISTFT to obtain  $\tilde{y}_s(t)$ .

**CodecSep (NAC latent-domain):**

$$x \xrightarrow{Enc(\cdot)} Z \in \mathbb{R}^{d \times T} \xrightarrow{Mask(Z, e_\tau)} \tilde{Z}_s = M_s \odot Z \xrightarrow{Dec(\cdot)} \tilde{y}_s(t),$$

with a frozen DAC backbone  $Enc(\cdot), Dec(\cdot)$ , and a FiLM-conditioned transformer masker  $Mask(\cdot, e_\tau)$  that estimates a soft mask  $M_s \in [0, 1]^{d \times T}$  conditioned on both the codec latents  $Z = Enc(x)$  and the text embedding  $e_\tau$ . The predicted mask  $M_s$  is applied element-wise to  $Z$  to produce source-specific latents  $\tilde{Z}_s = M_s \odot Z$ , which are subsequently decoded by  $Dec(\cdot)$  to obtain the separated waveform  $\tilde{y}_s(t)$ .

**Dimensionality reduction and compression.** For a typical 1s audio, 32 kHz STFT used by spectrogram-domain baselines, the mixture spectrogram  $X \in \mathbb{C}^{F \times T}$  (e.g.,  $F = 2 \cdot 1024, T \approx 100$ ) contains about  $|X| \approx 204,800$  complex coefficients. In contrast, a neural audio codec latent  $Z \in \mathbb{R}^{d \times T_c}$  is far more compact: at 16 kHz with  $d = 64$  and  $T_c = \frac{16000}{320} \approx 50$ ,  $|Z| = 3,200$ ; at 32 kHz with  $T_c = \frac{32000}{320} \approx 100$ ,  $|Z| = 6,400$ . Thus, the ratio  $|Z|/|X|$  is  $\approx 1.5625 \times 10^{-2}$  for 16 kHz and  $\approx 3.125 \times 10^{-2}$  for 32 kHz, implying a  $\sim 32\text{--}64\times$  reduction in representation size. Operating directly in  $Z$  therefore cuts memory bandwidth and MACs for the separator  $Mask(\cdot)$  while retaining perceptually salient structure imparted by the codec, making latent-domain separation both compute-efficient and semantically aligned. Moreover, the compact channel dimension ( $d = 64$ ) enables a smaller masker (fewer parameters in  $Q/K/V$  and MLP projections) and more effective self-attention.

#### 3.3.1 Why NAC latents (vs. spectrograms) and how the codec prior enables separation?

**STFT vs. NAC encoding.** The STFT is a *linear* projection from  $x(t)$  to  $X \in \mathbb{C}^{F \times T}$  and does not explicitly preserve or organize the intrinsic semantic structure of audio. Consequently, spectrogram-based separators (e.g., AudioSep) require an additional learned encoder-decoder (typically CNN/ResUNet) to first compress  $X$  into high-dimensional latent features and then decode spectrogram masks that are discriminatively trained for separation. This couples *semantic abstraction* and *separation* into one network, increasing parameters and MACs and forcing the model to learn structure “from scratch” in a redundant, noisy representation.

**NAC encoder as a semantic prior.** Neural audio codecs (DAC) are trained with perceptual, adversarial, and codebook objectives that encourage the encoder  $Enc(\cdot)$  to map  $x$  into compact, structured latents:

$$Enc(\cdot) : x \mapsto Z \in \mathbb{R}^{d \times T_c}.$$

These latents lie on a *discriminative compressed manifold*  $\mathcal{M}_{\text{latent}}$  in which semantically meaningful factors (e.g., pitch, timbre, transients) are disentangled and aligned for downstream use. In our system, we operate directly on the *continuous* latents  $Z$  (from  $Enc$ ), use a FiLM-conditioned transformer masker to predict a separation mask  $M_k$  from a textual query  $\tau_k$ , and form the estimate

$$\tilde{Z}_k = M_k \odot Z, \quad \tilde{y}_k = Dec(\tilde{Z}_k),$$

thereby leveraging the codec’s structured manifold for masking instead of learning a new representation.

**Separation mapping in latent vs. spectrogram space.** In CodecSep, the separator learns

$$Mask(\cdot, \cdot) : Z \in \mathcal{M}_{\text{latent}} \rightarrow \hat{Z}_k,$$

which is easier to optimize because the input is denoised, compressed, and semantically organized by the codec. In contrast, spectrogram models must learn

$$g(\cdot, \cdot) : X \in \mathbb{C}^{F \times T} \rightarrow \hat{Y}_k,$$

over a noisier, higher-dimensional space *without* semantic compression.

**Hierarchical (RVQ) structure that benefits separation.** The codec applies Residual Vector Quantization (RVQ) to  $Z$ , producing discrete codes  $A = [a_t \in [K]^{N_q}]_{t=1}^{T_c}$  with  $K = 1024$  and  $N_q$  quantizers. Codebook lookup yields embeddings

$$e_t = \sum_{i=1}^{N_q} \text{lookup}(a_t^{(i)}), \quad E = [e_t | t \in [T]] \approx Z,$$

and  $Dec(E)$  reconstructs the waveform. The RVQ cascade induces a natural coarse-to-fine hierarchy: the first quantizer captures coarse structure (e.g., low-frequency content, speaker/instrument timbre, global acoustic traits), while later quantizers refine residual details (e.g., high-frequency components, onsets/transients, background textures). This hierarchy mirrors the discriminative cues needed for separation and is directly exploitable by a mask-based transformer.

**Loss-induced organization of the latent space.** The DAC objective shapes  $Z$  using complementary terms:

- *Multi-scale spectral loss*  $\mathcal{L}_{\text{mel}}$  to preserve perceptually relevant frequency content at multiple time scales;
- *Time-domain reconstruction loss*  $\mathcal{L}_{\text{feat}} = \|x(t) - \tilde{y}(t)\|_1$  for fidelity and stability;
- *Multi-resolution adversarial loss*  $\mathcal{L}_{\text{adv}}$  with (i) multi-period waveform discriminators (pitch/periodicity) and (ii) multi-band STFT discriminators (fine spectral detail), plus a *feature-matching* term  $\mathcal{L}_{\text{feat}}^G$ ;
- *Codebook loss*  $\mathcal{L}_{\text{code}}$  to ensure compact, diverse, well-utilized codes and reinforce RVQ’s coarse-to-fine disentanglement.
- *Quantizer dropout (RVQ stage dropout)*: randomly disabling a subset of RVQ stages during training to discourage over-reliance on late codebooks and encourage smoother coarse-to-fine residual allocation, yielding more bitrate-robust and well-structured RVQ representations.

The overall loss is

$$\mathcal{L}_{\text{DAC}} = \lambda_{\text{mel}} \mathcal{L}_{\text{mel}} + \lambda_{\text{feat}} \mathcal{L}_{\text{feat}} + \lambda_{\text{adv}} \mathcal{L}_{\text{adv}} + \lambda_{\text{code}} \mathcal{L}_{\text{code}},$$

yielding latents that are (i) *denoised* (robust to low-level artifacts), (ii) *semantic* (preserve pitch, timbre, temporal structure), (iii) *disentangled* (coarse-to-fine RVQ), and (iv) *efficient* (bitrate-aware constraints).

**Separation benefits from the codec prior (and contrast to spectrogram baselines).** Because  $Z$  is already semantically organized, the FiLM-conditioned masker operates on a representation

that encodes the right factors for selection, not generation. This (i) reduces compute and memory (the separator acts on compact  $Z$  instead of  $X$ ), (ii) accelerates convergence and improves stability (masking over a clean manifold), and (iii) improves robustness to prompt variation (text FiLM modulates semantically aligned channels). In contrast, spectrogram systems must learn a task-specific latent from  $X$  and perform separation *jointly*, which increases parameter count and MACs, slows convergence, and can lead to overfitting in the absence of the codec’s inductive bias.

### 3.3.2 Transformer-based masker vs. decoder-style generation (specific design choice).

In CodecSep, we replace decoder-style source generation (as in CodecFormer, which directly predicts the target waveform/spectrogram) with a *Transformer-based, FiLM-conditioned masker* that outputs a soft mask over the codec latents. Concretely,

$$M_s = \text{Mask}(Z, e_\tau) \in [0, 1]^{d \times T}, \quad \tilde{Z}_s = M_s \odot Z, \quad \tilde{y}_s(t) = \text{Dec}(\tilde{Z}_s).$$

This choice has the following concrete advantages (all in the NAC latent domain):

- **Efficient and stable training.** Predicting  $M_s$  to *modulate* existing latent content is a simpler, more constrained learning problem than end-to-end *generation* of  $\tilde{Z}_s$  or  $\tilde{y}_s(t)$  with a decoder head. Working in  $Z$  avoids the instability commonly observed in direct waveform/spectrogram prediction, leading to faster convergence and lower training variance under the same optimization settings.
- **Minimal distortion through modulation (no hallucination).** The separator does not synthesize new content; it rescales and selects what is already encoded in  $Z$ . Forming  $\tilde{Z}_s = M_s \odot Z$  preserves the mixture’s latent structure and reduces artifacts relative to encoder-decoder separation pipelines that generate source signals from scratch, thereby limiting hallucinations and leakage.
- **Preservation of long-term temporal/spectral structure.** The NAC encoder has already organized periodicity, timbre, and transient structure in  $Z$ . Masking retains this organization across long contexts, whereas fully convolutional decoders trained to *generate* sources often exhibit long-term inconsistencies (e.g., drift over time or loss of periodic cues) when reconstructing from scratch.
- **Efficient use of Transformer capacity.** Instead of *synthesizing* source signals, the masker learns to *gate* semantically organized channels in  $Z$ , which is a substantially lighter optimization problem than decoder-style generation. FiLM conditioning steers the transformer to decide *where/how much* information to pass—not *what* to generate—so parameters and compute in the  $Q/K/V$  and MLP projections are concentrated on selection and attenuation.

### 3.3.3 Why We Integrated FiLM Conditioning into NAC-Based Separation

We deliberately integrate *Feature-wise Linear Modulation (FiLM)* Perez et al. [2018] *inside* the transformer masker to inject text semantics while preserving the codec manifold and keeping  $\text{Enc}(\cdot)/\text{Dec}(\cdot)$  frozen.

**Targeted placement (masker, mid-layers).** Given a CLAP text embedding  $e_\tau$ , a lightweight query network  $\text{query}(\cdot)$  produces per-layer affine parameters

$$(\gamma^l, \beta^l)_{l=1}^L = \text{query}(e_\tau), \quad \gamma^l, \beta^l \in \mathbb{R}^d,$$

which modulate intermediate activations  $H^l \in \mathbb{R}^{d \times T}$  for  $l \in \{2, \dots, L-1\}$ :

$$\tilde{H}_s^l = \text{FiLM}(H^l; \gamma^l, \beta^l) = \gamma^l \odot H^l + \beta^l.$$

Placing FiLM in the *masker* (not in *Enc* or *Dec*) keeps the codec latent distribution intact and confines conditioning to the *selection* step.

**Lightweight computation (overhead and parameterization).** FiLM adds only small per-layer vectors  $(\gamma^l, \beta^l)$  and a compact  $\text{query}(\cdot)$  MLP; it does *not* increase sequence length, attention heads, or the quadratic attention cost. The extra FLOPs/params are negligible relative to multi-head attention and MLP blocks, aligning with CodecSep’s efficiency goals.

**Non-iterative inference (single forward pass).** FiLM applies in a single pass through the masker. Unlike iterative conditioning mechanisms (e.g., flow-matching-based sampling), there are *no* sampling steps, thus preserving low latency for edge and hybrid deployments.

**Manifold preservation and stability.** Because FiLM scales/shifts existing channels of  $H^l$  rather than rewriting  $Z$  or generating  $\tilde{Z}_s$  from scratch, the NAC manifold structure (periodicity, timbre, transients) is preserved. Empirically this reduces training variance and mitigates long-horizon inconsistencies common with generator-style heads.

### 3.3.4 Why report results on $Z$ (continuous latents) and how to extend to code streams $A \rightarrow E$

**Why we evaluate on continuous latents  $Z$ .** We choose to perform—and therefore report—separation on the *continuous* DAC encoder latents  $Z = Enc(x) \in \mathbb{R}^{d \times T_c}$  for the following concrete reasons:

1. **End-to-end gradient flow for separation.** Our training updates only the masker and query networks while keeping the codec frozen. Using  $Z$  allows straightforward backpropagation through  $Mask(\cdot, e_\tau)$  and  $Dec(\cdot)$  without dealing with discrete indices or straight-through estimators; gradients are well-behaved and convergence is consistently stable.
2. **Representational fidelity and disentanglement.** During codec pretraining, the RVQ cascade *regularizes*  $Z$  so that pitch, timbre, onsets/transients, and background textures are cleanly and hierarchically organized.  $Z$  therefore provides a richer, more disentangled signal for FiLM-conditioned masking than hard code indices, which are subject to quantization coarsening.
3. **Training stability and variance.** In our setting (frozen codec), operating on  $Z$  avoids variability from codebook utilization dynamics (e.g., late-stage RVQ sensitivity, bitrate truncation). Empirically, this reduces run-to-run variance and removes the need for specialized regularizers when training the separator.

**How to extend the same model to discrete code streams.** For deployment scenarios where the input is a compressed bitstream, we operate on the *reconstructed embeddings*  $E$  obtained from the codes  $A$  via codebook lookup, and train the masker on  $E$  instead of  $Z$ :

$$A = [a_t \in [1024]^{N_q} \mid t \in [T_c]], \quad e_t = \sum_{i=1}^{N_q} \text{lookup}(a_t^{(i)}), \quad (5)$$

$$E = [e_t]_{t=1}^{T_c} \approx Z, \quad \tilde{E}_s = M_s \odot E, \quad \tilde{y}_s(t) = Dec(\tilde{E}_s) \quad (6)$$

**Compressed bitstream path (codes-in, codes-out).** Given  $E \approx Z$  and the element-wise masking operation, the estimated source embeddings satisfy

$$\tilde{E}_s = M_s \odot E \approx M_s \odot Z = Z_s$$

When a uniform codec pathway (or codes-out interface) is required, we re-quantize the masked embeddings and optionally decode via the codec:

$$\hat{A}_s = Quant(\tilde{E}_s), \quad \hat{E}_s = \text{lookup}(\hat{A}_s), \quad \tilde{y}_s(t) = Dec(\hat{E}_s)$$

In deployments that only need to return a bitstream, the server can emit  $\hat{A}_s$  directly and defer decoding to the client; otherwise, decoding  $Dec(\tilde{E}_s)$  or  $Dec(\hat{E}_s)$  yields the waveform on-device or server-side, respectively.

*Embedding alignment (CodecFormer-EL Yip et al. [2024a]).* To tighten  $\tilde{E}_s \approx Z_s$ , we can optimize an embedding-level consistency loss as in CodecFormer-EL Yip et al. [2024a] instead of our SI-SDR objective:

$$\mathcal{L}_{\text{emb}} = \sum_s \|\tilde{E}_s - Z_s\|_1$$

**Why this works.** By design of the codec,  $E$  approximates  $Z$  at the operating bitrate; the decoder already reconstructs  $\hat{x}(t) = Dec(E)$  with high fidelity. Since our separator is a *masker* (selective

modulation) rather than a generator, replacing  $Z$  with  $E$  preserves the semantics needed for separation while enabling direct operation on bitstreams. In practice, the extension amounts to training (or fine-tuning) the same FiLM-conditioned transformer on  $E$  with unchanged objectives.

**Summary of scope.** We present results on  $Z$  to (i) isolate separator performance without discrete-index training complications, (ii) leverage continuous gradient flow and stable optimization, and (iii) align FiLM conditioning with a smooth latent manifold. The deployment-ready path to discrete code streams is immediate: switch the masker input to  $E$  via lookup from  $A$  and train/fine-tune accordingly, with optional distribution alignment and bitrate-robustness augmentation.

### 3.3.5 Deployment advantages of CodecSep over spectrogram-domain separators (AudioSep)

**Central motivation.** In realistic deployments, edge devices already run a neural audio codec; they transmit *code streams* rather than raw waveforms. CodecSep treats the codec backbone as part of the separation stack and operates *directly* on codec representations, thereby eliminating redundant *decode*  $\rightarrow$  *separate*  $\rightarrow$  *re-encode* cycles required by spectrogram-domain systems.

**Pipeline comparison (server-side separation).** *Traditional (spectrogram) pipeline:*

$$\underbrace{\text{Edge: } \text{Enc}(\cdot)}_{\text{codec}} \Rightarrow \text{Code} \Rightarrow \underbrace{\text{Server: } \text{Dec}(\cdot) + g(\cdot, e_\tau) + \text{Enc}(\cdot)}_{\text{decode + separate + re-encode}} \Rightarrow \text{Code} \Rightarrow \text{Edge: } \text{Dec}(\cdot)$$

*CodecSep pipeline:*

$$\underbrace{\text{Edge: } \text{Enc}(\cdot)}_{\text{codec}} \Rightarrow \text{Code} \Rightarrow \underbrace{\text{Server: } \text{Mask}(\cdot, e_\tau)}_{\text{mask on } E \approx Z} \Rightarrow \text{Code} \Rightarrow \text{Edge: } \text{Dec}(\cdot)$$

CodecSep performs FiLM-modulated masking in the codec latent domain and returns separated code streams for edge-side decoding; spectrogram systems must decode to waveform (or magnitude/phase), separate in  $X$ , and re-encode.

**Complexity accounting.** Let  $C_{\text{enc}}$  and  $C_{\text{dec}}$  be codec encode/decode costs,  $C_{\text{spec}}$  the spectrogram separator cost, and  $C_{\text{mask}}$  the CodecSep masker cost.

**Code-stream input (typical):** AudioSep:  $C_{\text{dec}} + C_{\text{spec}} + C_{\text{enc}}$ , CodecSep:  $C_{\text{mask}}$ .

**Audio-stream input (edge-only):** AudioSep:  $C_{\text{spec}}$ , CodecSep:  $C_{\text{enc}} + C_{\text{mask}} + C_{\text{dec}}$ .

In the common (code-stream) case, CodecSep removes both decode and re-encode on the server. Moreover, *within* the separator, CodecSep operates on  $Z/E$  with  $|Z| \ll |X|$  (cf. Sec. 3.3), reducing activation memory and bandwidth throughout attention and MLP blocks.

**Interface compatibility with codec bitstreams.** When only quantized codes  $A = [a_t | t \in [T]]$  are available, we reconstruct embeddings by codebook lookup  $E = [e_t | t \in [T]]$  with  $e_t = \sum_{i=1}^{N_q} \text{lookup}(a_t^{(i)}) \approx Z$  and apply the same masker:

$$A \Rightarrow E \approx Z \xrightarrow{\text{Mask}(\cdot, e_\tau)} \tilde{E}_s \Rightarrow \text{Code stream out.}$$

No architectural change is required; separation remains in the codec latent domain and stays fully compatible with streaming/edge ecosystems.

**Why spectrogram-domain systems incur extra overhead.** Spectrogram separators (e.g., AudioSep) are defined on  $X = \text{STFT}(x)$ . Given code-stream inputs, they must first run  $\text{Dec}(\cdot)$  to obtain a waveform, compute  $X$ , perform separation, and then run  $\text{Enc}(\cdot)$  to return codes. This decode + separate + re-encode loop adds latency, memory traffic, and energy cost on the server path and scales poorly with concurrent streams.

### Operational advantages of CodecSep.

- **Eliminates redundant codec cycles in server workflows:** With code streams, we reconstruct embeddings  $E \approx Z$  by codebook lookup (Sec. 3.3.4), avoiding server-side decode/re-encode; only the edge decodes the final stems.

- **Smaller working representation during separation:** masking in  $Z/E$  (e.g.,  $d=64$ ) reduces intermediate activations, lowering memory bandwidth and enabling tighter batching.
- **Non-iterative, single-pass conditioning:** FiLM-conditioning within the masker adds negligible overhead and preserves low latency (no iterative sampling).
- **Seamless edge/server hybrid and edge-only modes:** identical separator logic serves both modalities; with code-stream inputs, the server path remains *separator-only*.
- **Maintains codec manifold structure:** by modulating  $Z/E$  rather than rebuilding  $X$ , CodecSep preserves periodicity/timbre/transients already organized by the codec, supporting stable, high-fidelity stems at deployment.

## 4 Experiments

### 4.1 Datasets

#### 4.1.1 Divide and Remaster v 2.0 (dnr-v2)

dnr-v2 Petermann et al. [2022] dataset consists of 60s-duration artificial mixtures of speech, music, and SFX sampled from LibriSpeech Panayotov et al. [2015], Free Music Archive (FMA) Defferrard et al. [2017], and Freesound Dataset 50K (FSD50K) Fonseca et al. [2022], respectively. It includes 3,406 (56.7hrs) training, 487 (8.13hrs) validation, and 973 (16.22hrs) test mixtures, each provided with its three individual source audios. The mixtures are generated by normalizing each source to fixed Loudness Units Full-Scale (LUFS) levels:  $-17$  dB (speech),  $-24$  dB (music), and  $-21$  dB (SFX), with  $\pm 2$  dB random perturbations. Any source exceeding a peak threshold is normalized to 0.5 dB. The sources are mixed and normalized to  $-27$  dB LUFS with additional random perturbations. The validation and test sets are trimmed for silence and split into 5s or 10s segments. Segments where sources are present for less than 50% of the duration are removed, resulting in 2,852 ( $\approx 3.96$ hrs) validation and 1,840 ( $\approx 5.11$ hrs) test mixtures.

While originally developed for 3-stem separation, we adapt dnr-v2 to the USS setting by replacing fixed source labels with natural language descriptions. For speech or music stem, we use broad, category-level prompts (e.g., “speech,” “music”), reflecting realistic usage in production workflows. In contrast, SFX sources are more complex—often containing three or more overlapping events. We generate prompts to query the SFX stem using FSD50K’s hierarchical annotations, combining fine-grained class labels with their parent categories. This results in long-form, compositional queries that reflect the structure of the mixture (e.g., “dog barking, Animal, engine rumbling, motor vehicle”).

#### 4.1.2 Open-Domain Benchmarks

We benchmark on five open-domain datasets spanning captioned audio, environmental sounds, and large multi-event corpora: **AudioCaps** Kim et al. [2019], an AudioSet-derived collection of  $> 46k$  10 s YouTube clips paired with human-written captions describing the dominant sound events (used by us to synthesize training and test mixtures); **ESC-50** Piczak, a curated environmental sound dataset of 2,000 clips (5 s each) organized into 50 classes with 40 examples per class across five meta-categories (animals, natural, human non-speech, domestic, exterior/urban); **Clotho-v2** Drossos et al. [2020], 6,974 audio samples (15–30 s) each annotated with five human captions (8–20 words) covering open-domain events; **AudioSet-eval** Gemmeke et al. [2017], the evaluation split of AudioSet comprising human-labeled 10 s YouTube clips over an ontology of 632 audio event classes in a multi-label setting; and **VGGSound** Chen et al. [2020a], an AudioSet-derived audio–visual corpus with 550+ hours of 10 s segments covering a wide variety of everyday sound categories. For AudioCaps we form both training and testing mixtures by summing three clips (validation segmented into 5 s, test preserves clips up to 20 s), while for ESC-50, Clotho-v2, AudioSet-eval, and VGGSound we construct test-only mixtures using the same three-clip protocol.

### 4.2 Evaluation

We evaluate CodecSep alongside TDANet Li et al. [2023], Pons et al. [2024], CodecFormer Yip et al. [2024b], SDCodec Bie et al. [2024], and AudioSep Liu et al. [2024] on universal source separation conducted on the dnr-v2 and AudioCaps test splits. We report the scale-invariant signal-to-distortion ratio (SI-SDR) Luo and Mesgarani [2019], Le Roux et al. [2019] for signal quality assessment and

Table 1: Results: Separation Performance, Universal Source Separation (**dnr-v2-test**)

Model	Metric ( $\uparrow$ )	Separation		
		Music	Speech	Sfx
AudioSep (zero-shot)	SI-SDR	$-2.46^{\pm 4.06}$	$4.92^{\pm 4.21}$	$-0.34^{\pm 5.39}$
	ViSQOL	$2.86^{\pm 0.63}$	$3.11^{\pm 0.56}$	<b><math>2.63^{\pm 0.77}</math></b>
AudioSep + dnr-v2	SI-SDR	$-5.55^{\pm 2.89}$	$7.68^{\pm 3.0}$	$-4.66^{\pm 3.68}$
	ViSQOL	$2.59^{\pm 0.57}$	$2.49^{\pm 0.37}$	$2.32^{\pm 0.7}$
<b>CodecSep + dnr-v2</b>	SI-SDR	<b><math>1.15^{\pm 3.29}</math></b>	<b><math>9.97^{\pm 2.92}</math></b>	<b><math>0.89^{\pm 4.22}</math></b>
	ViSQOL	<b><math>2.86^{\pm 0.57}</math></b>	<b><math>3.14^{\pm 0.45}</math></b>	$2.33^{\pm 0.73}$
<b>CodecSep + dnr-v2</b> (ablate Masker)	SI-SDR	$-6.72^{\pm 2.77}$	$1.95^{\pm 2.84}$	$-6.75^{\pm 3.83}$
	ViSQOL	$2.48^{\pm 0.58}$	$2.58^{\pm 0.50}$	$2.08^{\pm 0.74}$
AudioSep + AudioCaps (zero-shot)	SI-SDR	$-14.86^{\pm 23.08}$	$-7.11^{\pm 25.80}$	$-14.63^{\pm 23.26}$
	ViSQOL	$2.36^{\pm 0.71}$	$2.43^{\pm 0.70}$	$2.15^{\pm 0.79}$
<b>CodecSep + AudioCaps</b> (zero-shot)	SI-SDR	$-8.46^{\pm 2.78}$	$2.47^{\pm 2.91}$	$-5.93^{\pm 4.33}$
	ViSQOL	$2.27^{\pm 0.53}$	$2.56^{\pm 0.47}$	$2.06^{\pm 0.72}$

Virtual Speech Quality Objective Listener (ViSQOL) Chinen et al. [2020] for perceptual quality assessment. ViSQOL Chinen et al. [2020] evaluates the perceptual similarity between the ground truth  $x$  and the estimated signal  $\tilde{x}$  using a spectro-temporal approach. It then predicts a Mean Opinion Score - Listening Quality Objective (MOS-LQO), which ranges from 1 (lowest quality) to 5 (highest quality). In addition, we evaluate the inference efficiency of our models in a hardware-agnostic setting by reporting Multiply-and-Accumulate operations (MACs) using Torchprofile<sup>1</sup> averaged over 8 audios of 2s duration each.

### 4.3 Training

The complete model, including the query module  $query(\cdot)$ , is trained for  $400K$  iterations with DAC Kumar et al. [2023] and CLAP Wu et al. [2023] modules frozen. Validation is conducted every  $5K$  iterations and test every  $10K$  iterations. We use ADAM Kingma and Ba [2017] as our optimizer and train with a batch size of 4 examples, each 2 seconds in duration, and a learning rate of  $1.5e^{-4}$  on a single 24GB NVIDIA A-30 GPU. Training employs a *ReduceLRonPlateau* Mukherjee et al. [2019] scheduler, which reduces the learning rate by a factor of 0.5 if the validation loss does not improve for two consecutive validation checks. We train two versions of CodecSep, one using the dnr-v2 dataset and the other using AudioCaps, to evaluate performance across different training distributions. We refer to these models using the prefixes +dnr-v2 and +AudioCaps, respectively, to indicate which dataset each model was trained on.

Since TDANet and CodecFormer were originally developed for speech separation, we re-trained newly initialized versions on the dnr-v2 training set using the same configuration as CodecSep. For AudioSep, we evaluate the publicly available pre-trained model—trained on diverse datasets—and versions re-trained on dnr-v2 and AudioCaps using our setup for consistency. We also include SDCodec, using the official pre-trained models made available by the authors. To ensure a fair comparison, all inputs to TDANet and AudioSep undergo codec processing during training and inference. This accounts for codec-induced distortions and artifacts, reflecting realistic deployment scenarios where audio is typically processed through compression pipelines in cloud-based systems.

### 4.4 Results and Discussions

Tables 1–6 present universal source separation results, prompt–granularity analyses, architectural ablations, cross-dataset generalization, paraphrase robustness, and full inference complexity under matched training/evaluation protocols. Table 1 reports dnr-v2 test results for speech, music, and SFX: text-guided models use generic prompts for speech/music and ground-truth compositional

<sup>1</sup><https://github.com/zhijian-liu/torchprofile.git>

captions for SFX; we also include a masker ablation to isolate the role of the Transformer masker. Table 2 studies SFX prompt granularity across three regimes—(i) fixed-stem, non-text baselines (TDANet, CodecFormer, SDCodec), (ii) generic 3-stem prompts ( $\{\text{music, speech, sfx}\}$ ), and (iii) a universal setup with fine-grained, compositional SFX prompts—thereby aligning input conditions for fair comparison with fixed-head systems. Table 3 isolates architecture: decoder-style generation (CodecFormer) vs. an unguided 3-stem masker variant and its text-guided counterpart, all operating in the codec latent space. To assess out-of-domain generalization, Table 4 evaluates on AudioCaps-test with mixtures of three randomly sampled sources and prompts drawn from captions (not tied to fixed labels). Beyond AudioCaps/dnr-v2, Table 5 benchmarks on four additional open-domain corpora (ESC-50, Clotho-v2, AudioSet-eval, VGGSound) under the same prompt protocol. Table 6 probes prompt paraphrasing robustness by replacing the generic speech/music prompts with unseen synonymous variants at inference (zero-shot paraphrase test). Finally, Table 7 compares end-to-end and architecture-only GMACs for spectrogram-domain separation versus codec-latent masking, including the practical code-stream case. All models are evaluated against the original (uncompressed) ground truth; our methods are highlighted in **bold**; and we report mean and standard deviation ( $1\sigma$ ) over each evaluation set.

**Source Separation Performance on dnr-v2 (Table 1).** CodecSep+dnr-v2 outperforms both pre-trained AudioSep (zero-shot scenario) and retrained AudioSep+dnr-v2 across all categories, with significant SI-SDR gains in speech (9.97 vs. 4.92/ 7.68 dB), music (1.15 vs. -2.46/ -5.55 dB), and SFX (0.89 vs. -0.34/ -4.66 dB). Regarding VisQOL, CodecSep matches or exceeds AudioSep in speech and music but slightly underperforms in SFX. While AudioSep is trained on a diverse dataset with sfx prompts covering isolated events and complex mixtures, CodecSep is trained exclusively on long-form, compositional SFX prompts from dnr-v2. Despite this narrower prompt exposure, CodecSep remains robust and achieves the highest overall SI-SDR. As part of our ablation study, we evaluate a lightweight variant—CodecSep+dnr-v2 (ablate Masker)—that removes the transformer masker and applies text conditioning directly to the encoder. While it performs comparable to AudioSep+dnr-v2 in SI-SDR, it achieves better perceptual quality for speech. The drop in separation quality stems from FiLM distorting the encoder’s latent space, which holds the mixture representation.

**Effect of SFX Prompt Granularity during training (Table 2).** We evaluate three regimes: (i) *fixed-stem* baselines without text guidance (TDANet, CodecFormer, SDCodec), (ii) *generic 3-stem* prompts (“music/speech/sfx”), and (iii) *universal* prompting that retains generic cues for speech/music but uses fine-grained, compositional SFX descriptions. Across settings, CodecSep is competitive with or stronger than fixed-stem baselines on SFX while maintaining comparable speech/music quality, despite those baselines being explicitly supervised per head. Under matched generic-prompt training/evaluation, CodecSep remains robust and surpasses the spectrogram-domain AudioSep, indicating that effective separation does not hinge on carefully crafted prompts. Moreover, replacing the single “sfx” label with detailed SFX prompts consistently sharpens SFX extraction and, importantly, improves speech and music stems as well—suggesting that richer SFX supervision enhances overall scene disentanglement. While these controlled studies cover multiple prompt granularities, we expect additional gains from training on larger, more diverse corpora with a spectrum of prompt specificities, which we leave for future work.

**Why use a Transformer masker instead of a decoder? (Table 3).** We compare (i) CodecFormer (decoder-style source generation), (ii) CodecSep (unguided, 3-stem) which uses the CodecFormer Transformer as a masker over codec latents, and (iii) CodecSep (text-guided). The results on **dnr-v2-test** exhibit two clear trends. First, replacing decoder-style generation with masking consistently strengthens separation across music, speech, and SFX. This aligns with our design rationale: in the DAC latent domain, the masker modulates existing, semantically structured content instead of synthesizing new signals, which (a) reduces artifacts and cross-talk leakage, (b) preserves long-range periodicity/timbre and transient organization already encoded by the codec, and (c) stabilizes optimization compared to end-to-end generation. Second, adding text guidance yields a further uniform improvement. The masker formulation concentrates Transformer capacity on selection (“where/how much” to pass) rather than generation (“what” to produce). Taken together, these findings support our design choice: in the codec latent space, a FiLM-conditioned Transformer masker is a more effective and robust allocator of model capacity than a decoder, with text guidance further sharpening that allocation.

**Generalization across open-domain datasets.** Table 4 reports generalization results on the AudioCaps-test set derived from AudioSet. AudioSep benefits from distributional alignment, having

Table 2: Results: Impact of SFX Prompt Granularity on Universal Source Separation (**dnr-v2-test**)

Model	Metric ( $\uparrow$ )	Separation		
		Music	Speech	Sfx
<b>3-Stem: Fixed stem baselines (no text-guidance)</b>				
TDANet	SI-SDR	1.84 $\pm$ 3.55	10.18 $\pm$ 2.91	1.36 $\pm$ 4.90
	ViSQOL	2.85 $\pm$ 0.58	3.09 $\pm$ 0.43	2.44 $\pm$ 0.72
CodecFormer	SI-SDR	-5.67 $\pm$ 3.44	2.27 $\pm$ 2.32	-6.54 $\pm$ 4.36
	ViSQOL	2.16 $\pm$ 0.47	2.51 $\pm$ 0.49	2.13 $\pm$ 0.67
SDCodec	SI-SDR	<b>1.85<math>\pm</math>3.68</b>	<b>11.32<math>\pm</math>2.98</b>	<b>1.77<math>\pm</math>4.08</b>
	ViSQOL	<b>2.96<math>\pm</math>0.56</b>	<b>3.49<math>\pm</math>0.40</b>	<b>2.64<math>\pm</math>0.73</b>
<b>3-Stem: {"music", "speech", "sfx"} as generic prompt</b>				
AudioSep (zero-shot)	SI-SDR	<b>-2.46<math>\pm</math>4.06</b>	4.92 $\pm$ 4.21	-6.65 $\pm$ 4.73
	ViSQOL	<b>2.86<math>\pm</math>0.63</b>	<b>3.11<math>\pm</math>0.56</b>	2.08 $\pm$ 0.68
AudioSep + dnr-v2	SI-SDR	-6.22 $\pm$ 2.77	<b>7.71<math>\pm</math>3.11</b>	-2.11 $\pm$ 3.90
	ViSQOL	2.55 $\pm$ 0.57	2.47 $\pm$ 0.37	2.39 $\pm$ 0.74
<b>CodecSep + dnr-v2</b>	SI-SDR	-7.71 $\pm$ 2.84	4.63 $\pm$ 2.48	<b>0.58<math>\pm</math>4.15</b>
	ViSQOL	2.45 $\pm$ 0.55	2.70 $\pm$ 0.49	<b>2.39<math>\pm</math>0.70</b>
<b>Universal: {"music", "speech", fine-grained sfx prompt}</b>				
AudioSep (zero-shot)	SI-SDR	-2.46 $\pm$ 4.06	4.92 $\pm$ 4.21	-0.34 $\pm$ 5.39
	ViSQOL	2.86 $\pm$ 0.63	3.11 $\pm$ 0.56	<b>2.63<math>\pm</math>0.77</b>
AudioSep + dnr-v2	SI-SDR	-5.55 $\pm$ 2.89	7.68 $\pm$ 3.0	-4.66 $\pm$ 3.68
	ViSQOL	2.59 $\pm$ 0.57	2.49 $\pm$ 0.37	2.32 $\pm$ 0.7
<b>CodecSep + dnr-v2</b>	SI-SDR	<b>1.15<math>\pm</math>3.29</b>	<b>9.97<math>\pm</math>2.92</b>	<b>0.89<math>\pm</math>4.22</b>
	ViSQOL	<b>2.86<math>\pm</math>0.57</b>	<b>3.14<math>\pm</math>0.45</b>	2.33 $\pm$ 0.73

Table 3: Results: Architectural advantages in using CodecFormer decoder as masker (**dnr-v2-test**)

Model	Metric ( $\uparrow$ )	Separation		
		Music	Speech	Sfx
CodecFormer	SI-SDR	-5.67 $\pm$ 3.44	2.27 $\pm$ 2.32	-6.54 $\pm$ 4.36
	ViSQOL	2.16 $\pm$ 0.47	2.51 $\pm$ 0.49	2.13 $\pm$ 0.67
<b>CodecSep + dnr-v2</b> (unguided, 3-stem)	SI-SDR	1.15 $\pm$ 3.35	9.90 $\pm$ 2.91	0.82 $\pm$ 4.18
	ViSQOL	2.75 $\pm$ 0.55	3.09 $\pm$ 0.45	<b>2.48<math>\pm</math>0.72</b>
<b>CodecSep + dnr-v2</b> (text-guided)	SI-SDR	<b>1.15<math>\pm</math>3.29</b>	<b>9.97<math>\pm</math>2.92</b>	<b>0.89<math>\pm</math>4.22</b>
	ViSQOL	<b>2.86<math>\pm</math>0.57</b>	<b>3.14<math>\pm</math>0.45</b>	2.33 $\pm$ 0.73

Table 4: Results: Generalization, Universal Source Separation (**AudioCaps-test**)

Model	Separation	
	SI-SDR ( $\uparrow$ )	ViSQOL ( $\uparrow$ )
AudioSep	-2.51 $\pm$ 12.14	<b>2.44<math>\pm</math>1.08</b>
AudioSep + dnr-v2 (zero-shot)	-6.44 $\pm$ 11.48	2.33 $\pm$ 1.08
<b>CodecSep + dnr-v2</b> (zero-shot)	<b>-6.09<math>\pm</math>11.62</b>	2.24 $\pm$ 1.16
AudioSep + AudioCaps	-9.17 $\pm$ 18.71	2.29 $\pm$ 1.11
<b>CodecSep + AudioCaps</b>	<b>-6.19<math>\pm</math>10.58</b>	2.14 $\pm$ 1.00

Table 5: Results: Further Benchmarking on **ESC-50**, **Clotho-v2**, **AudioSet-eval**, **VGGSound**

Model	Metric ( $\uparrow$ )	Separation			
		ESC-50	Clotho-v2	AudioSet-eval	VGGSound
AudioSep + dnr-v2	SI-SDR	$-7.75^{\pm 14.46}$	$-8.57^{\pm 17.0}$	$-7.62^{\pm 11.42}$	$-7.03^{\pm 12.65}$
	ViSQOL	$2.29^{\pm 1.12}$	$2.09^{\pm 1.08}$	$2.09^{\pm 1.00}$	$2.22 \pm 1.10$
<b>CodecSep + dnr-v2</b>	SI-SDR	$-5.87^{\pm 11.55}$	$-6.02^{\pm 11.10}$	$-6.37^{\pm 10.53}$	$-6.12^{\pm 12.12}$
	ViSQOL	$2.34^{\pm 1.13}$	$2.14^{\pm 1.09}$	$2.15^{\pm 1.0}$	$2.25^{\pm 1.11}$

been trained on diverse datasets, including AudioSet, and consequently achieves the strongest separation performance. CodecSep+dnr-v2 generalizes well to AudioCaps and outperforms AudioSep+dnr-v2 in SI-SDR while maintaining competitive ViSQOL scores. When retrained on AudioCaps, CodecSep again outperforms AudioSep in separation quality, demonstrating strong cross-domain robustness. Table 1 further supports this trend on the more challenging dnr-v2 test set, where CodecSep+AudioCaps outperforms AudioSep+AudioCaps in SI-SDR across all sources while maintaining comparable perceptual quality. However, both models experience a performance drop on dnr-v2 due to its increased mixture complexity, often containing speech, music, and three or more overlapping SFX sources—making it significantly more challenging than the simpler mixtures seen during AudioCaps training.

**Further benchmarking on ESC-50, Clotho-v2, AudioSet-eval, and VGGSound (Table 5).** Extending beyond AudioCaps and dnr-v2, we evaluate both systems on four additional open-domain benchmarks spanning environmental sound classification (ESC-50), audio captioning-style corpora (Clotho-v2), weakly labeled web-scale audio (AudioSet-eval), and visually grounded audio (VGGSound). Under matched training data and prompt protocols, **CodecSep+dnr-v2** consistently outperforms **AudioSep+dnr-v2** across all four datasets in both separation fidelity and perceptual quality. Taken together with the dnr-v2 analyses, these results indicate that CodecSep’s latent-domain masking—leveraging the codec’s structured, semantically aligned representations—confers robust cross-domain behavior while using  $25\times$  less architecture-only compute than spectrogram separators. This combination of accuracy and efficiency is particularly attractive in practical deployments, where models must generalize to diverse sound taxonomies under strict compute and memory budgets.

**Robustness to prompt paraphrasing (Table 6) .** To probe lexical sensitivity, we re-evaluated both CodecSep + dnr-v2 and AudioSep + dnr-v2 on the **dnr-v2** test split by replacing the generic training-time prompts for *speech* and *music* with three unseen paraphrases per class—*speech*: {“spoken voice”, “human conversation”, “people talking”}; *music*: {“instrumental music”, “band playing”, “melody with instruments”}. This constitutes a zero-shot paraphrase generalization test: models are trained with generic category cues but must respond to synonymous, potentially broader descriptors at inference. We observe a consistent qualitative pattern: (i) both systems exhibit the expected degradation when moving from generic to paraphrased prompts, confirming that lexical ambiguity weakens query–audio alignment; (ii) CodecSep degrades more gracefully overall, maintaining stronger separation and perceptual quality for *speech*, and retaining a small but persistent advantage for *music*; and (iii) the gap between models narrows under paraphrasing, yet the relative ranking is preserved, suggesting that FiLM-conditioned masking over structured codec latents confers robustness to synonym-level shifts. Notably, this study isolates lexical paraphrases; we did not incorporate paraphrases with explicit temporal qualifiers (e.g., “applause follows a song”), which we leave to future work.

**Full inference complexity (Table 7) .** We compare end-to-end GMACs for spectrogram-domain separation (AudioSep) and our codec-latent approach (CodecSep). *Code-stream input (typical deployment)*: when the server receives codec bitstreams, CodecSep runs a masker-only path and costs just 1.35 GMACs, whereas AudioSep must decode, separate, and re-encode, totaling 73.6 GMACs—about a  $54\times$  compute reduction in favor of CodecSep. *Architecture-only (separator compute, excluding codec)*: CodecSep remains at 1.35 GMACs versus 33.5 GMACs for AudioSep ( $\approx 25\times$  lower), reflecting the smaller working representation in the codec latent space. *Audio-stream input*: if the server is fed raw audio, CodecSep incurs the codec overhead ( $Enc(\cdot) = 12.28$  GMACs,  $Dec(\cdot) = 27.82$  GMACs), yielding 41.45 GMACs end-to-end versus 33.5 GMACs for AudioSep; these codec costs disappear in the code-stream setting. Practically, even on the edge, full-band waveform processing is rarely feasible under memory constraints; audio is typically encoded to codes precisely

Table 6: Results: Impact of prompt ambiguity (**dnr-v2-test**)

Model	Metric ( $\uparrow$ )	Separation	
		Music	Speech
<b>Using Generic Prompts for Speech and Music</b>			
AudioSep + dnr-v2	SI-SDR	$-5.55^{\pm 2.89}$	$7.68^{\pm 3.0}$
	ViSQOL	$2.59^{\pm 0.57}$	$2.49^{\pm 0.37}$
<b>CodecSep + dnr-v2</b>	SI-SDR	$1.15^{\pm 3.29}$	$9.97^{\pm 2.92}$
	ViSQOL	$2.86^{\pm 0.57}$	$3.14^{\pm 0.45}$
<b>Using ambiguous prompts for Speech and Music</b>			
AudioSep + dnr-v2	SI-SDR	$-6.43^{\pm 3.29}$	$4.14^{\pm 3.77}$
	ViSQOL	$2.53^{\pm 0.57}$	$2.64^{\pm 0.47}$
<b>CodecSep + dnr-v2</b>	SI-SDR	$-5.60^{\pm 3.61}$	$4.19^{\pm 4.18}$
	ViSQOL	$2.56^{\pm 0.58}$	$2.74^{\pm 0.51}$

Table 7: Full Inference Complexity (GMACs  $\downarrow$ )

Model	Input: Audio Stream	Input: Code Stream	Architecture-only
AudioSep	33.5	73.6	33.5
<b>CodecSep</b>	41.45	$1.35 (\downarrow 54\times)$	$1.35 (\downarrow 25\times)$
<i>Codec GMACs used above: DAC Enc(.) = 12.28, Dec(.) = 27.82.</i>			

to reduce footprint and bandwidth. Consequently, code-stream processing is the operational default, for which CodecSep is purpose-built.

**Relative-gain summaries (Appendix A).** For a compact view of percent improvements, Appendix A Table 8 reports relative gains of CodecSep over AudioSep under matched training data and prompt protocols, complementing the absolute results in the main text. In brief: on **dnr-v2**, CodecSep yields large improvements in SI-SDR with clear perceptual lifts; under **paraphrased prompts**, gains are smaller but remain positive, indicating robustness to lexical variation; across **ESC-50**, **Clotho-v2**, **AudioSet-eval**, and **VGGSound**, SI-SDR gains are consistent while ViSQOL deltas are modest; and when **trained on AudioCaps**, CodecSep maintains an advantage on AudioCaps-test and shows strong improvements when evaluated on dnr-v2.

**Reconstruction study (Appendix B).** We probe *source leakage* with a *single-source reconstruction* diagnostic on dnr-v2-test : each input contains one target source and models are either prompted with the matching class/label (text-guided) or routed to the corresponding fixed head (non-text-guided). We also report *mixture reconstruction* by summing predicted source stems for a mixture and comparing to the original. This is a leakage/consistency check—not a primary separation metric; full setup/results are in the Appendix B (Table 9).

## 5 Conclusion

CodecSep delivers state-of-the-art text-guided source separation while operating directly in the codec latent domain, yielding consistently stronger separation than AudioSep across dnr-v2 and five additional open-domain datasets, and doing so with markedly lower computational cost. The results in Tables 1–6 support three core findings. First, replacing decoder-style generation with a Transformer *masker* over codec latents materially improves separation quality; text guidance provides a further uniform boost. Second, CodecSep generalizes competitively beyond its training distribution (AudioCaps, ESC-50, Clotho-v2, AudioSet-eval, VGGSound), and degrades more gracefully under prompt paraphrasing than a spectrogram-domain baseline. Third, in the deployment-relevant code-stream regime, CodecSep’s masker-only path reduces end-to-end GMACs by  $\sim 54\times$  (and  $\sim 25\times$  *architecture-only*), aligning accuracy with practical efficiency.

**Limitations and clarifications.** (1) *Codec/bandwidth.* Our experiments use a 16 kHz mono NAC for reproducibility and on-device feasibility; however, *CodecSep* is *codec-agnostic*. The masker operates on continuous NAC latents with a frozen codec, so upgrading to 44.1/48 kHz and/or stereo is a drop-in backbone swap with no architectural changes to masking or conditioning. (2) *Data and prompts.* Training data scale and prompt diversity are modest relative to open-domain audio. As shown in Table 2, finer SFX supervision sharpens SFX extraction *and* improves speech/music stems; larger, more heterogeneous corpora spanning multiple prompt granularities—including temporal/relational cues—should yield further gains. (3) *Temporal prompting.* While *CodecSep* is robust to synonymous paraphrases, we did not evaluate prompts with explicit temporal structure (e.g., causal ordering), which remains an open direction. (4) *Perceptual SFX quality.* In some settings, SFX perceptual quality trails the best competing scores despite superior SI-SDR; improving SFX naturalness without sacrificing separation is future work. (5) *Perceptual evaluation.* Following *CodecFormer*, we report ViSQL as a proxy for listening quality (predicting MOS-LQO on a 1–5 scale). Although we did not conduct a formal multi-listener study, we include real-world audio outputs for both *CodecSep* and *AudioSep* in the supplementary material, together with a Markdown summary of an informal author listening pass.

**Future Works.** We will scale *CodecSep* with higher-bandwidth/stereo codecs, broaden prompt coverage (including temporal and referring-expression cues), explore stronger self-alignment objectives, and investigate alternative conditioning (audio-only or multimodal) within the same FiLM-masking framework. Combined with its large compute reduction and code-stream compatibility, these extensions position *CodecSep* as a practical foundation for fast, universal, and deployable prompt-guided source separation.

## References

Xiaoyu Bie, Xubo Liu, and Gaël Richard. Learning source disentanglement in neural audio codec. *arXiv preprint arXiv:2409.11228*, 2024.

Zalán Borsos, Raphaël Marinier, Damien Vincent, Eugene Kharitonov, Olivier Pietquin, Matt Sharifi, Dominik Roblek, Olivier Teboul, David Grangier, Marco Tagliasacchi, and Neil Zeghidour. Audioltm: a language modeling approach to audio generation, 2023. URL <https://arxiv.org/abs/2209.03143>.

Honglie Chen, Weidi Xie, Andrea Vedaldi, and Andrew Zisserman. Vggsound: A large-scale audio-visual dataset. In *ICASSP 2020-2020 IEEE International Conference on Acoustics, Speech and Signal Processing (ICASSP)*, pages 721–725. IEEE, 2020a.

Jingjing Chen, Qirong Mao, and Dong Liu. Dual-path transformer network: Direct context-aware modeling for end-to-end monaural speech separation. *arXiv preprint arXiv:2007.13975*, 2020b.

Michael Chinen, Felicia S. C. Lim, Jan Skoglund, Nikita Gureev, Feargus O’Gorman, and Andrew Hines. Visql v3: An open source production ready objective speech and audio metric, 2020. URL <https://arxiv.org/abs/2004.09584>.

Michaël Defferrard, Kirell Benzi, Pierre Vandergheynst, and Xavier Bresson. Fma: A dataset for music analysis, 2017. URL <https://arxiv.org/abs/1612.01840>.

Alexandre Défossez, Nicolas Usunier, Léon Bottou, and Francis R. Bach. Music source separation in the waveform domain. *CoRR*, abs/1911.13254, 2019. URL <http://arxiv.org/abs/1911.13254>.

Jacob Devlin, Ming-Wei Chang, Kenton Lee, and Kristina Toutanova. Bert: Pre-training of deep bidirectional transformers for language understanding, 2019. URL <https://arxiv.org/abs/1810.04805>.

Konstantinos Drossos, Samuel Lipping, and Tuomas Virtanen. Clotho: An audio captioning dataset. In *ICASSP 2020-2020 IEEE International Conference on Acoustics, Speech and Signal Processing (ICASSP)*, pages 736–740. IEEE, 2020.

Zhihao Du, Jiaming Wang, Qian Chen, Yunfei Chu, Zhifu Gao, Zerui Li, Kai Hu, Xiaohuan Zhou, Jin Xu, Ziyang Ma, Wen Wang, Siqi Zheng, Chang Zhou, Zhijie Yan, and Shiliang Zhang. Lauragpt: Listen, attend, understand, and regenerate audio with gpt, 2024. URL <https://arxiv.org/abs/2310.04673>.

Alexandre Défossez, Nicolas Usunier, Léon Bottou, and Francis Bach. Music source separation in the waveform domain, 2021. URL <https://arxiv.org/abs/1911.13254>.

Alexandre Défossez, Jade Copet, Gabriel Synnaeve, and Yossi Adi. High fidelity neural audio compression, 2022. URL <https://arxiv.org/abs/2210.13438>.

Eduardo Fonseca, Xavier Favory, Jordi Pons, Frederic Font, and Xavier Serra. Fsd50k: An open dataset of human-labeled sound events, 2022. URL <https://arxiv.org/abs/2010.00475>.

Jort F. Gemmeke, Daniel P. W. Ellis, Dylan Freedman, Aren Jansen, Wade Lawrence, R. Channing Moore, Manoj Plakal, and Marvin Ritter. Audio set: An ontology and human-labeled dataset for audio events. In *Proc. IEEE ICASSP 2017*, New Orleans, LA, 2017.

Romain Hennequin, Anis Khelif, Felix Voituret, and Manuel Moussallam. Spleeter: a fast and efficient music source separation tool with pre-trained models. *Journal of Open Source Software*, 5(50):2154, 2020.

Yanxin Hu, Yun Liu, Shubo Lv, Mengtao Xing, Shimin Zhang, Yihui Fu, Jian Wu, Bihong Zhang, and Lei Xie. Dccrn: Deep complex convolution recurrent network for phase-aware speech enhancement. *arXiv preprint arXiv:2008.00264*, 2020.

Ilya Kavalerov, Scott Wisdom, Hakan Erdogan, Brian Patton, Kevin Wilson, Jonathan Le Roux, and John R. Hershey. Universal sound separation. In *2019 IEEE Workshop on Applications of Signal Processing to Audio and Acoustics (WASPAA)*, pages 175–179, 2019. doi: 10.1109/WASPAA.2019.8937253.

Chris Dongjoo Kim, Byeongchang Kim, Hyunmin Lee, and Gunhee Kim. Audiocaps: Generating captions for audios in the wild. In *NAACL-HLT*, 2019.

Diederik P. Kingma and Jimmy Ba. Adam: A method for stochastic optimization, 2017. URL <https://arxiv.org/abs/1412.6980>.

Rithesh Kumar, Prem Seetharaman, Alejandro Luebs, Ishaan Kumar, and Kundan Kumar. High-fidelity audio compression with improved rvqgan. In A. Oh, T. Naumann, A. Globerson, K. Saenko, M. Hardt, and S. Levine, editors, *Advances in Neural Information Processing Systems*, volume 36, pages 27980–27993. Curran Associates, Inc., 2023. URL [https://proceedings.neurips.cc/paper\\_files/paper/2023/file/58d0e78cf042af5876e12661087bea12-Paper-Conference.pdf](https://proceedings.neurips.cc/paper_files/paper/2023/file/58d0e78cf042af5876e12661087bea12-Paper-Conference.pdf).

Jonathan Le Roux, Scott Wisdom, Hakan Erdogan, and John R Hershey. Sdr-half-baked or well done? In *ICASSP 2019-2019 IEEE International Conference on Acoustics, Speech and Signal Processing (ICASSP)*, pages 626–630. IEEE, 2019.

Kai Li, Runxuan Yang, and Xiaolin Hu. An efficient encoder-decoder architecture with top-down attention for speech separation, 2023. URL <https://arxiv.org/abs/2209.15200>.

Xubo Liu, Qiuqiang Kong, Yan Zhao, Haohe Liu, Yi Yuan, Yuzhuo Liu, Rui Xia, Yuxuan Wang, Mark D. Plumbley, and Wenwu Wang. Separate anything you describe, 2024. URL <https://arxiv.org/abs/2308.05037>.

Yi Luo and Nima Mesgarani. Conv-tasnet: Surpassing ideal time–frequency magnitude masking for speech separation. *IEEE/ACM Transactions on Audio, Speech, and Language Processing*, 27(8):1256–1266, August 2019. ISSN 2329-9304. doi: 10.1109/taslp.2019.2915167. URL <http://dx.doi.org/10.1109/TASLP.2019.2915167>.

Koyel Mukherjee, Alind Khare, and Ashish Verma. A simple dynamic learning rate tuning algorithm for automated training of dnns, 2019. URL <https://arxiv.org/abs/1910.11605>.

Vassil Panayotov, Guoguo Chen, Daniel Povey, and Sanjeev Khudanpur. Librispeech: An asr corpus based on public domain audio books. In *2015 IEEE International Conference on Acoustics, Speech and Signal Processing (ICASSP)*, pages 5206–5210, 2015. doi: 10.1109/ICASSP.2015.7178964.

Ethan Perez, Florian Strub, Harm de Vries, Vincent Dumoulin, and Aaron Courville. Film: Visual reasoning with a general conditioning layer. *Proceedings of the AAAI Conference on Artificial Intelligence*, 32(1), Apr. 2018. doi: 10.1609/aaai.v32i1.11671. URL <https://ojs.aaai.org/index.php/AAAI/article/view/11671>.

Darius Petermann, Gordon Wichern, Zhong-Qiu Wang, and Jonathan Le Roux. The cocktail fork problem: Three-stem audio separation for real-world soundtracks. In *ICASSP 2022 - 2022 IEEE International Conference on Acoustics, Speech and Signal Processing (ICASSP)*, pages 526–530, 2022. doi: 10.1109/ICASSP43922.2022.9746005.

Karol J. Piczak. ESC: Dataset for Environmental Sound Classification. In *Proceedings of the 23rd Annual ACM Conference on Multimedia*, pages 1015–1018. ACM Press. ISBN 978-1-4503-3459-4. doi: 10.1145/2733373.2806390. URL <http://dl.acm.org/citation.cfm?doid=2733373.2806390>.

Jordi Pons, Xiaoyu Liu, Santiago Pascual, and Joan Serrà. Gass: Generalizing audio source separation with large-scale data. In *ICASSP 2024 - 2024 IEEE International Conference on Acoustics, Speech and Signal Processing (ICASSP)*, pages 546–550, 2024. doi: 10.1109/ICASSP48485.2024.10446601.

Daniel Stoller, Sebastian Ewert, and Simon Dixon. Wave-u-net: A multi-scale neural network for end-to-end audio source separation. *arXiv preprint arXiv:1806.03185*, 2018.

Cem Subakan, Mirco Ravanelli, Samuele Cornell, Mirko Bronzi, and Jianyu Zhong. Attention is all you need in speech separation. In *ICASSP 2021-2021 IEEE International Conference on Acoustics, Speech and Signal Processing (ICASSP)*, pages 21–25. IEEE, 2021.

Naoya Takahashi, Nabarun Goswami, and Yuki Mitsuji. Mmdenselstm: An efficient combination of convolutional and recurrent neural networks for audio source separation. In *2018 16th International workshop on acoustic signal enhancement (IWAENC)*, pages 106–110. IEEE, 2018.

Emmanuel Vincent, Tuomas Virtanen, and Sharon Gannot. *Audio source separation and speech enhancement*. John Wiley & Sons, 2018.

Chengyi Wang, Sanyuan Chen, Yu Wu, Ziqiang Zhang, Long Zhou, Shujie Liu, Zhuo Chen, Yanqing Liu, Huaming Wang, Jinyu Li, Lei He, Sheng Zhao, and Furu Wei. Neural codec language models are zero-shot text to speech synthesizers, 2023. URL <https://arxiv.org/abs/2301.02111>.

Xiaofei Wang, Manthan Thakker, Zhuo Chen, Naoyuki Kanda, Sefik Emre Eskimez, Sanyuan Chen, Min Tang, Shujie Liu, Jinyu Li, and Takuya Yoshioka. Speechx: Neural codec language model as a versatile speech transformer, 2024. URL <https://arxiv.org/abs/2308.06873>.

Scott Wisdom, Efthymios Tzinis, Hakan Erdogan, Ron Weiss, Kevin Wilson, and John Hershey. Unsupervised sound separation using mixture invariant training. *Advances in neural information processing systems*, 33:3846–3857, 2020.

Yusong Wu, Ke Chen, Tianyu Zhang, Yuchen Hui, Taylor Berg-Kirkpatrick, and Shlomo Dubnov. Large-scale contrastive language-audio pretraining with feature fusion and keyword-to-caption augmentation. In *ICASSP 2023 - 2023 IEEE International Conference on Acoustics, Speech and Signal Processing (ICASSP)*, pages 1–5, 2023. doi: 10.1109/ICASSP49357.2023.10095969.

Jia Qi Yip, Chin Yuen Kwok, Bin Ma, and Eng Siong Chng. Speech separation using neural audio codecs with embedding loss, 2024a. URL <https://arxiv.org/abs/2411.17998>.

Jia Qi Yip, Shengkui Zhao, Dianwen Ng, Eng Siong Chng, and Bin Ma. Towards audio codec-based speech separation, 2024b. URL <https://arxiv.org/abs/2406.12434>.

Dong Yu, Morten Kolbæk, Zheng-Hua Tan, and Jesper Jensen. Permutation invariant training of deep models for speaker-independent multi-talker speech separation. In *2017 IEEE International Conference on Acoustics, Speech and Signal Processing (ICASSP)*, pages 241–245. IEEE, 2017.

Neil Zeghidour, Alejandro Luebs, Ahmed Omran, Jan Skoglund, and Marco Tagliasacchi. Sound-stream: An end-to-end neural audio codec. *IEEE/ACM Transactions on Audio, Speech, and Language Processing*, 30:495–507, 2022. doi: 10.1109/TASLP.2021.3129994.

Liu Ziyin, Tilman Hartwig, and Masahito Ueda. Neural networks fail to learn periodic functions and how to fix it. In H. Larochelle, M. Ranzato, R. Hadsell, M.F. Balcan, and H. Lin, editors, *Advances in Neural Information Processing Systems*, volume 33, pages 1583–1594. Curran Associates, Inc., 2020. URL [https://proceedings.neurips.cc/paper\\_files/paper/2020/file/1160453108d3e537255e9f7b931f4e90-Paper.pdf](https://proceedings.neurips.cc/paper_files/paper/2020/file/1160453108d3e537255e9f7b931f4e90-Paper.pdf).

Table 8: Relative gains (%) of **CodecSep** over **AudioSep** under matched training/prompt settings. Each sub-table reports percent improvements for a specific evaluation setup.

(a) DnR-v2 test set			(b) Ambiguous prompts (speech & music paraphrases)		
Metric	Relative Gain (%)			Metric	Relative Gain (%)
	Speech	Music	SFX		Speech
SI-SDR	+29.8	+120.7	+119.1	SI-SDR	+1.2
ViSQOL	+26.1	+10.5	+0.5	ViSQOL	+3.8

(c) Additional open-domain benchmarks					
Metric	AudioCaps	ESC-50	Clotho-v2	AudioSet	VGGSound
SI-SDR	+5.5	+24.3	+30.0	+16.4	+13.0
ViSQOL	-4.3	+2.2	+2.4	+2.9	+2.9

(d) Training on AudioCaps					
Metric	AudioCaps-test	dnR-v2			
		Music	Speech	SFX	
SI-SDR	+32.5	+43.1	+134.7	+59.5	
ViSQOL	-6.5	-3.8	+5.4	-4.2	

## A Discussion of Relative-Gain Summaries.

Tables 8a–8d consolidate *relative* improvements of **CodecSep** over **AudioSep** under matched training data and prompt protocols, complementing the absolute results in the main text. On **DnR-v2** (Table 8a), CodecSep delivers large SI-SDR gains—especially for music and SFX—together with a clear perceptual lift. Under **paraphrased prompts** (Table 8b), gains are smaller but remain positive, indicating robustness to lexical variation. Across **additional open-domain benchmarks** (Table 8c), SI-SDR gains are consistent while ViSQOL deltas are modest, aligning with cross-domain trends reported earlier. Finally, when **trained on AudioCaps** (Table 8d), CodecSep maintains an advantage on AudioCaps-test and yields strong improvements on DnR-v2, supporting the claim that codec-latent masking generalizes well across datasets and prompt regimes.

Table 9: Results: Reconstruction Performance, Universal Source Separation (**dnr-v2-test**)

Model	Metric ( $\uparrow$ )	Reconstruction			
		Mixture	Music	Speech	Sfx
<b>3-Stem: Fixed Stem, Non Text-guided</b>					
TDANet	SI-SDR	$-3.26^{\pm 7.78}$	<b>7.96<math>^{\pm 5.29}</math></b>	<b>11.07<math>^{\pm 3.32}</math></b>	<b>4.70<math>^{\pm 5.11}</math></b>
	ViSQOL	$3.93^{\pm 0.35}$	<b>4.20<math>^{\pm 0.46}</math></b>	<b>4.51<math>^{\pm 0.32}</math></b>	<b>4.09<math>^{\pm 0.39}</math></b>
CodecFormer	SI-SDR	$-47.55^{\pm 9.51}$	$-47.11^{\pm 10.97}$	$-47.77^{\pm 9.65}$	$-48.21^{\pm 9.87}$
	ViSQOL	$1.02^{\pm 0.07}$	$1.04^{\pm 0.12}$	$1.01^{\pm 0.06}$	$1.16^{\pm 0.47}$
<b>CodecSep + dnr-v2</b> <b>(unguided, 3-stem)</b>	SI-SDR	$3.42^{\pm 1.85}$	$4.12^{\pm 3.97}$	$6.15^{\pm 2.87}$	$0.83^{\pm 5.16}$
	ViSQOL	$3.23^{\pm 0.20}$	$3.02^{\pm 0.33}$	$3.47^{\pm 0.24}$	$3.23^{\pm 0.46}$
SDCodec	SI-SDR	<b>6.98<math>^{\pm 2.49}</math></b>	$7.65^{\pm 4.60}$	$8.28^{\pm 3.26}$	$2.54^{\pm 5.65}$
	ViSQOL	<b>4.29<math>^{\pm 0.15}</math></b>	$4.03^{\pm 0.28}$	$4.44^{\pm 0.15}$	$3.98^{\pm 0.34}$
<b>Text-guided</b>					
AudioSep (zero-shot)	SI-SDR	$5.53^{\pm 1.96}$	$4.69^{\pm 5.36}$	$10.97^{\pm 2.99}$	$-1.99^{\pm 5.68}$
	ViSQOL	$4.06^{\pm 0.38}$	$3.75^{\pm 0.65}$	$4.57^{\pm 0.13}$	$3.19^{\pm 0.77}$
AudioSep + dnr-v2	SI-SDR	$6.47^{\pm 2.26}$	$7.99^{\pm 4.55}$	$8.13^{\pm 3.35}$	$2.29^{\pm 5.95}$
	ViSQOL	$4.20^{\pm 0.18}$	$4.12^{\pm 0.21}$	$3.03^{\pm 0.29}$	$3.81^{\pm 0.47}$
<b>CodecSep + dnr-v2</b>	SI-SDR	$4.06^{\pm 2.06}$	$3.91^{\pm 3.93}$	$6.10^{\pm 2.86}$	$0.67^{\pm 5.29}$
	ViSQOL	$3.74^{\pm 0.22}$	$3.37^{\pm 0.33}$	$3.83^{\pm 0.24}$	$3.54^{\pm 0.44}$
<b>CodecSep + dnr-v2</b> (ablate Masker)	SI-SDR	<b>12.24<math>^{\pm 2.42}</math></b>	<b>12.58<math>^{\pm 3.81}</math></b>	<b>13.59<math>^{\pm 2.59}</math></b>	<b>8.67<math>^{\pm 4.17}</math></b>
	ViSQOL	<b>4.44<math>^{\pm 0.14}</math></b>	<b>4.13<math>^{\pm 0.31}</math></b>	<b>3.85<math>^{\pm 0.34}</math></b>	$3.76^{\pm 0.54}$
AudioSep + AudioCaps (zero-shot)	SI-SDR	$6.67^{\pm 2.52}$	$8.10^{\pm 4.63}$	$8.39^{\pm 3.21}$	$2.42^{\pm 6.12}$
	ViSQOL	$4.23^{\pm 0.19}$	$4.12^{\pm 0.21}$	$4.17^{\pm 0.21}$	<b>3.82<math>^{\pm 0.46}</math></b>
<b>CodecSep + AudioCaps</b> (zero-shot)	SI-SDR	$0.59^{\pm 1.89}$	$-0.24^{\pm 5.15}$	$-11.03^{\pm 5.21}$	$1.23^{\pm 4.84}$
	ViSQOL	$3.33^{\pm 0.23}$	$2.91^{\pm 0.64}$	$1.69^{\pm 0.48}$	$3.44^{\pm 0.41}$

## B Further Studies: Reconstruction Performance.

Table 9 assesses performance under a single-source reconstruction setting on the dnr-v2-test set, where each model is prompted to reproduce the input source. In addition, we report mixture reconstruction scores obtained by summing the separated sources and comparing them to the original mixture.

Among non-text-guided models, TDANet yields the best single-source reconstruction, while SDCodec performs better on mixture reconstruction. Replacing decoder-style *generation* in CodecFormer with a Transformer *masker* over codec latents in CodecSep+ dnr-v2, (unguided 3-stem) markedly improves both per-stem and mixture reconstruction fidelity and perceptual quality. Masking modulates information already organized in the codec manifold ( $Z$ ) rather than re-synthesizing it from scratch, avoiding collapse/artifacts and yielding tighter mixture consistency.

Among the text-guided models, CodecSep achieves reconstruction performance comparable to the pre-trained and retrained AudioSep variants across all source types. AudioSep consistently excels in reconstruction due to its STFT-based masking pipeline, which enables more controlled and artifact-free waveform synthesis. However, CodecSep surpasses the pretrained AudioSep in SFX reconstruction—across both SI-SDR and ViSQOL on dnr-v2. Notably, the masker ablated CodecSep variant delivers the best reconstruction performance on dnr-v2. With isolated single-source input and matching prompts, direct conditioning minimally disturbs the NAC latent space, allowing high-fidelity reconstruction in this variant. However, strong mixture reconstruction despite poor separation suggests source leakage across separated outputs.